

# HIGH ENERGY EMISSION OF GRB 130427A: EVIDENCE FOR INVERSE COMPTON RADIATION

YI-ZHONG FAN<sup>1</sup>, P.H.T. TAM<sup>2</sup>, FU-WEN ZHANG<sup>1</sup>, YUN-FENG LIANG<sup>3</sup>, HAO-NING HE<sup>1</sup>, BEI ZHOU<sup>1,4</sup>, RUI-ZHI YANG<sup>1,4</sup>,  
ZHI-PING JIN<sup>1</sup>, AND DA-MING WEI<sup>1</sup>

<sup>1</sup> Key Laboratory of Dark Matter and Space Astronomy, Purple Mountain Observatory, Chinese Academy of Science, Nanjing, 210008, China.

<sup>2</sup> Institute of Astronomy and Department of Physics, National Tsing Hua University, Hsinchu 30013, Taiwan.

<sup>3</sup> Department of Physics, Guangxi University, Guangxi 530004, China. and

<sup>4</sup> Graduate University of Chinese Academy of Sciences, Yuquan Road 19, Beijing, 100049, China.

*Draft version March 21, 2019*

## ABSTRACT

A nearby super-luminous burst GRB 130427A was simultaneously detected by five  $\gamma$ -ray space telescopes (*Swift*, Fermi-GBM/LAT, Konus-Wind, SPI-ACS/INTEGRAL and AGILE) and by three RAPTOR full-sky persistent monitors. The isotropic  $\gamma$ -ray energy release is of  $\sim 10^{54}$  erg and the absence of a jet break in the X-ray afterglow lightcurve up to  $t > 7$  days suggests an intrinsic energy release of  $> 10^{52}$  erg, rendering it the most powerful explosion among the GRBs with a redshift  $z \leq 0.5$ . The emission above 100 MeV lasted about one day and four photons are at energies greater than 40 GeV. We show that the count rate of 100 MeV-100 GeV emission may be mainly accounted for by the forward shock synchrotron radiation and the inverse Compton radiation likely dominates at GeV-TeV energies. In particular, an inverse Compton radiation origin is established for the  $\sim (95.3, 47.3, 41.4)$  GeV photons arriving at  $t \sim (243, 256.3, 610.6)$  s after the trigger of Fermi-GBM. Interestingly, the external-inverse-Compton-scattering of the prompt emission (the second episode, i.e.,  $t \sim 120 - 260$  s) by the forward-shock-accelerated electrons is expected to produce a few  $\gamma$ -rays with a typical energy  $\sim 10$  GeV, while five photons above 10 GeV were detected in the same time interval. A possible unified model for the prompt soft  $\gamma$ -ray, optical and GeV emission of GRB 130427A, GRB 080319B and GRB 090902B is outlined. Implication of the null detection of  $> 1$  TeV neutrinos from GRB 130427A by IceCube is discussed.

*Subject headings:* Gamma rays: general—Radiation mechanisms: non-thermal

## 1. INTRODUCTION

The high-energy ( $\geq 100$  MeV) emission properties of Gamma-ray Bursts (GRBs) can help us to better understand the physical composition of the GRB outflow, the radiation mechanisms, and possibly also the underlying physical processes shaping the early afterglow (see Fan & Piran 2008 and Zhang & Mészáros 2004 for reviews). For example, the inverse Compton radiation from GRB forward shock can extend to the very high energy ( $\epsilon_\gamma > 50$  GeV) range, while the synchrotron radiation can only give rise to emission up to  $\sim 10$  GeV ( $\Gamma/100$ ), where  $\Gamma$  is the bulk Lorentz factor of the GRB blast wave and drops with time quickly. Hence at  $t > 10^2$  s, usually we do not expect tens-GeV  $\gamma$ -rays coming from the synchrotron radiation of the forward shock. Therefore the detection of very high energy emission of GRBs at a fairly early time can impose a very tight constraint on the radiation mechanism. However, the very high energy photons are rare and are attenuated by the cosmic infrared/optical background before reaching us. Xue et al. (2009) investigated the detection prospect of very high energy emission of GRBs and found out that with current ground-based Cherenkov detectors, only for those very bright and nearby bursts like GRB 030329, detection of very high energy photons is possible under favorable observing conditions and a delayed observation time of  $\leq 10$  hr. Very bright and nearby bursts are very rare and for the ground-based detectors the observation conditions are not under control. That's why so far no positive detection of very high energy emission from GRBs

by the ground-based Cherenkov detectors has been reported, yet (e.g., Albert et al. 2007; Horan et al. 2007; Aharonian et al. 2009; Jarvis et al. 2010; Acciari et al. 2011).

In comparison with the ground-based Cherenkov detectors, the space telescopes such as EGRET onboard CGRO, GRID onboard AGILE, and the Large Area Telescope (LAT) onboard the Fermi satellite have a much smaller effective area. However these telescopes have a low energy threshold  $\sim$  tens MeV and can monitor the high energy emission since the trigger of some GRBs when the high energy emission flux is expected to be much higher than that at late times. Since 1994, tens GRBs with high energy emission had been reported. In the pre-Fermi-LAT era, the record of the most energetic  $\gamma$ -ray from GRBs is the  $\sim 18$  GeV photon following GRB 940217 (Hurley et al. 1994). The most energetic photon detected by Fermi-LAT till March 2013 is the 33.4 GeV  $\gamma$ -ray from GRB 090902B at a redshift  $z = 1.822$  (Abdo et al. 2009b, 2013). Such a record has been broken by GRB 130427A, a burst simultaneously detected by *Swift* (Maselli et al. 2013), Fermi Gamma-Ray Telescope (Zhu et al. 2013a; Kienlin et al. 2013), Konus-Wind (Golenetskii et al. 2013), SPI-ACS/INTEGRAL (Pozanenko et al. 2013), AIGLE (Verrecchia et al. 2013) and three RAPTOR full-sky persistent monitors (Wren et al. 2013). The highest energy LAT photon has an energy of  $> 90$  GeV (Zhu et al. 2013a). The redshift of this burst was measured to be  $0.3399 \pm 0.0002$  (Flores et al. 2013;

Levan et al. 2013; Xu et al. 2013). Its isotropic energy release is  $E_{\gamma, \text{iso}} \sim 1.05 \times 10^{54}$  erg (Amati et al. 2013), rendering it the most energetic one among the GRBs with a redshift  $z \leq 0.5$  detected so far (see Tab.1).

The prompt emission of GRB 130427A lasted a few hundred seconds and overlapped with the forward shock region significantly. The forward shock protons and electrons are also cooled by the prompt emission and high energy neutrinos and  $\gamma$ -rays are powered by the ultra-high energy protons interacting with the prompt  $\gamma$ -rays and by the electrons inverse-Compton-scattering off the prompt emission (Fan et al. 2005a,b). As a result of the Klein-Nishina suppression, the forward shock electrons are mainly cooled by the X-ray photons (Fan et al. 2005b, Wang et al. 2006). Therefore in section 2 we analyze the Swift BAT data and then extrapolate the 0.3-10 keV flux of the prompt emission. The 100MeV-100 GeV photon flux and the arrival time of the  $> 1$  GeV photons of GRB 130427A are also presented. In section 3 we examine the models of the long-lasting GeV emission. In section 3 we discuss the physical origin of the prompt emission. In section 5 we summarize our work with some discussion.

## 2. THE PROMPT 0.3-10 KEV EMISSION AND THE 100MEV-100GEV EMISSION

In this work  $T_0$  denotes the trigger of Fermi-GBM at 07:47:06.42 UT on 27 April 2013 (Kienlin et al. 2013). The *Swift* BAT was executing a pre-planned slew, so it was not triggered on time. But in the BAT lightcurve the main large peak started about 50 s before its trigger (Maselli et al. 2013; Barthelmy et al. 2013), consistent with the observations of Fermi-GBM, Konus-Wind, SPI-ACS/INTEGRAL and AGILE.

*The prompt 0.3-10 keV emission.* The BAT quick-look data were analyzed using the standard BAT analysis software distributed within HEASOFT 6.13 and the latest calibration files. The BAT ground-calculated position is RA= 173.150, Dec= 27.706 deg. Mask-tagged BAT count-rate light curve was extracted in the standard 15-150 keV energy bands, and converted to 15-150 keV flux with the energy conversion factor inferred from the spectral fitting in different time-intervals shown in Fig.1, where a simple power-law model is adopted. Assuming the spectrum is unchanged in the energy range 0.3 – 10 keV, the prompt X-ray emission lightcurve is extrapolated (see Fig.1).

*The 100 MeV - 100 GeV emission.* The first reports of the LAT emission were made by Zhu et al. (2013a, b). To better understand the high-energy emission we analyzed the LAT data that are available at the Fermi Science Support Center<sup>1</sup>, using the Fermi Science Tools v9r27p1 package. Events of energies between 100 MeV and 100 GeV were used. To reduce the contamination from Earth albedo  $\gamma$ -rays, we excluded events with zenith angles greater than  $100^\circ$ . Since we focused our work in the extended LAT emission that lasts for nearly a day, events classified as “P7SOURCE” and the instrument response functions “P7SOURCE\_V6” were used.

Events from a region-of-interest (ROI) of a  $20^\circ$ -radius circular region centered on the enhanced XRT position of GRB 130427A (GCN 14467) were analyzed

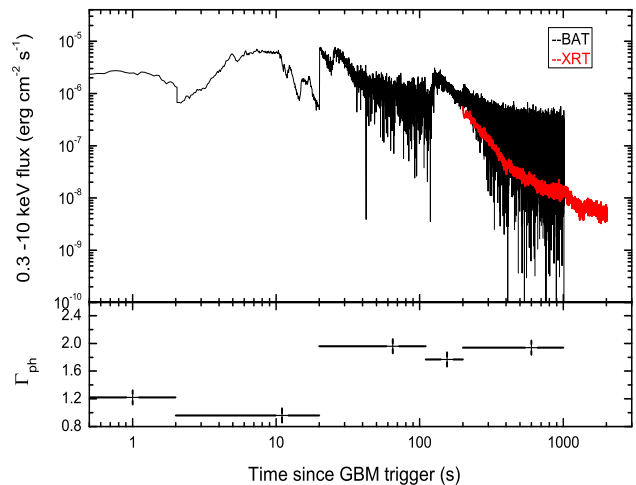


FIG. 1.— Upper panel: prompt 0.3 – 10 keV emission of GRB 130427A extrapolated from the BAT data. The red line is the XRT lightcurve taken from [http://www.swift.ac.uk/xrt\\_curves/00554620/](http://www.swift.ac.uk/xrt_curves/00554620/) (Evans et al. 2009). Lower panel: the photon index ( $\Gamma_{\text{ph}}$ ) of the prompt emission detected by BAT in different intervals.

using unbinned likelihood analyzes. The Galactic diffuse emission (gal\_2yearp7v6\_v0.fits) and the isotropic diffuse component (iso\_p7v6source.txt), as well as sources in the second Fermi catalog were included in the background model. However, it was shown that an isotropic component is enough to describe the background photons in the time bins before  $T_0 + 1000$  s, due to the dominance of the GRB emission over other sources in the ROI during these short-duration intervals.

We proceeded to construct a light curve in the energy interval 100 MeV to 100 GeV, using unbinned likelihood analyzes of each time bin. The light curve is shown in Fig.2. Due to the brightness of the GRB, intervals were as short as 5–10 seconds in the early times, e.g., before  $T_0 + 50$  s. As already noted in Zhu et al. (2013b), there is a possible break at around  $T_0 + 500$  s. Spectral analyzes on two time intervals:  $T_0$  to  $T_0 + 138$  s and  $T_0 + 138$  s to  $T_0 + 70$  ks were carried out. Assuming single power laws for the spectra of the GRB seen in the whole LAT range, no obvious spectral change was seen in between the two phases.

In Fig.3 we also present the photon energies and arrival times of the photons (to increase the photon statistics, a looser selection criterion: “P7TRANSIENT” is employed here) above 1 GeV since the trigger of Fermi GBM. The 95% contamination angle of LAT at 1 GeV is about  $3^\circ$ , that’s why in our plot only the photons within the  $3^\circ$  aperture have been taken into account.

## 3. PHYSICAL ORIGINS OF THE GEV EMISSION

At  $t > 500$  s the X-ray afterglow emission drops with time as  $\sim t^{-1.25}$  and the XRT spectrum is  $F_\nu \propto \nu^{-0.79 \pm 0.17}$  ([http://www.swift.ac.uk/xrt\\_curves/00554620/](http://www.swift.ac.uk/xrt_curves/00554620/); Evans et al. 2009). While the optical observations suggest a

<sup>1</sup> <http://fermi.gsfc.nasa.gov/ssc/>

TABLE 1  
THE OBSERVATIONAL PROPERTIES OF LOW REDSHIFT GRBs ( $z < 0.5$ )

| GRB     | $z$    | $E_{\text{peak}}^{\text{a}}$<br>(keV) | $E_{\gamma,\text{iso}}$<br>( $10^{51}$ erg) | Ref. <sup>b</sup> |
|---------|--------|---------------------------------------|---|-------------------|
| 990712  | 0.434  | $93 \pm 15$                           | $6.7 \pm 1.3$                               | 1                 |
| 980425  | 0.0085 | $122 \pm 17$                          | $9 \times 10^{-4}$                          | 2                 |
| 010921  | 0.45   | $129 \pm 26$                          | $9.5 \pm 1$                                 | 1                 |
| 011121  | 0.36   | $1060 \pm 265$                        | $78 \pm 21$                                 | 1                 |
| 020819B | 0.41   | $70 \pm 21$                           | $6.8 \pm 1.7$                               | 1                 |
| 020903  | 0.25   | $3.37 \pm 1.79$                       | $0.024 \pm 0.006$                           | 1                 |
| 030329  | 0.168  | $100 \pm 23$                          | $15 \pm 3$                                  | 1                 |
| 031203  | 0.105  | $> 190$                               | 0.17  | 2                 |
| 050709  | 0.1606 | $97.4 \pm 11.6$                       | $0.033 \pm 0.001$                           | 1                 |
| 060218  | 0.0331 | $4.9 \pm 0.3$                         | $0.053 \pm 0.003$                           | 3                 |
| 060505  | 0.089  | $> 160$                               | $0.03 \pm 0.01$                             | 3                 |
| 060614  | 0.125  | $55 \pm 45$                           | $2.5 \pm 1$                                 | 1                 |
| 061006  | 0.4377 | $955 \pm 267$                         | $2 \pm 0.3$                                 | 1                 |
| 061021  | 0.346  | $1046 \pm 485$                        | $4.6 \pm 0.8$                               | 1                 |
| 071227  | 0.383  | $1384 \pm 277$                        | $1 \pm 0.2$                                 | 1                 |
| 090417B | 0.345  | —                                     | $> 6.3$                                     | 4                 |
| 091127  | 0.49   | $51 \pm 1.5$                          | $16.1 \pm 0.3$                              | 1                 |
| 100316D | 0.0591 | $18^{+3}_{-2}$                        | 0.06  | 2                 |
| 120422A | 0.283  | $\sim 53$                             | 0.045                                       | 2                 |
| 130427A | 0.3399 | $1250 \pm 150$                        | $1050 \pm 150$                              | 5                 |

(<sup>a</sup>) The peak energy of the prompt emission in the burst frame.

(<sup>b</sup>) References: (1) Zhang et al. 2012b and references therein, (2) Zhang et al. 2012a, (3) Amati et al. 2007, (4) Holland et al. 2010, (5) Amati et al. 2013

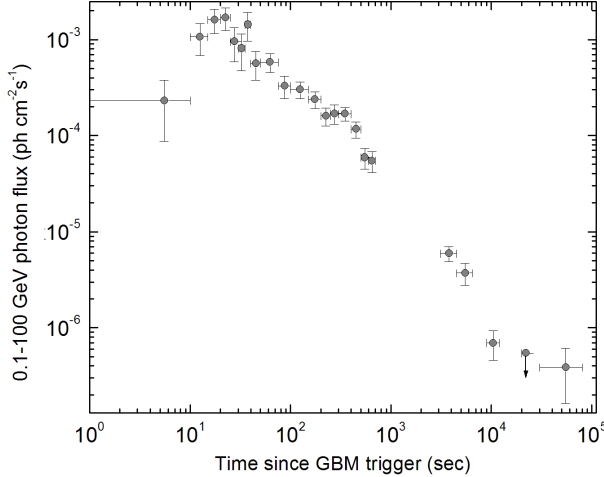


FIG. 2.— The 0.1-100 GeV photon flux of GRB 130427A.

shallower decline  $\sim t^{-1}$  (Zheng et al. 2013). Within the standard afterglow model, these data can be explained if the forward shock is in the slow cooling phase and the optical emission is below the cooling frequency but above the typical synchrotron radiation frequency of the forward shock while the X-ray band is above both (Piran 1999; Mészáros 2002; Zhang & Mészáros 2004). The number density of the circum-burst medium should be a constant (i.e.,  $n \sim \text{const.}$ ) and the power-law distribution index of the shock-accelerated electrons is  $p \sim 2.2$ . The absence of a clear jet break up to  $t > 7$  days suggests a half-opening angle of (Piran 1999)

$$\theta_j > 0.17 E_{\text{k},54}^{-1/8} n_0^{1/8} (t/7 \text{ d})^{3/8} [(1+z)/1.34]^{-3/8},$$

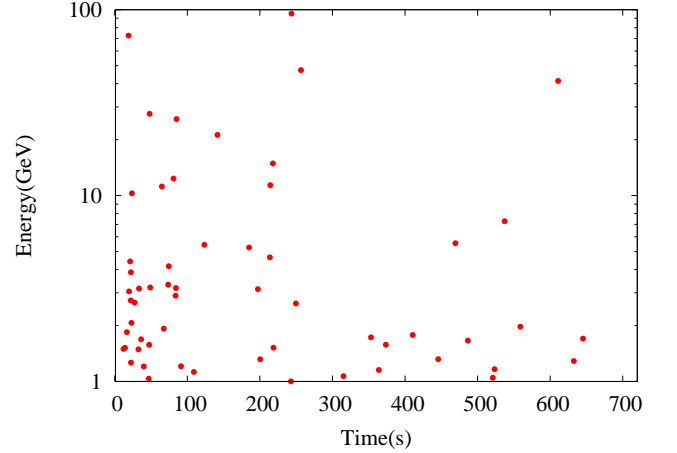


FIG. 3.— The arrival time of the  $\geq 1$  GeV photons after the trigger.

and the intrinsic  $\gamma$ -ray energy release of the ejecta is

$$E_{\gamma,\text{jet}} > 1.6 \times 10^{52} \text{ erg} \left( \frac{E_{\gamma,\text{iso}}}{1.05 \times 10^{54} \text{ erg}} \right) E_{\text{k},54}^{-1/4} n_0^{1/4} \left( \frac{t}{7 \text{ d}} \right)^{3/4},$$

where  $E_{\text{k}}$  is the isotropic-equivalent kinetic energy of the GRB ejecta. Here and throughout this text, the convention  $Q_{\text{x}} = Q/10^{\text{x}}$  has been adopted in CGS units except for specific notation.

### 3.1. The role of synchrotron radiation

The forward shock synchrotron radiation of some extremely bright GRBs can play the dominant role in producing  $< 10$  GeV emission, as firstly demonstrated by Zou et al. (2009, Fig.3 therein) just before the release of the first Fermi-LAT result on GeV afterglow emission.

Now such a scenario has been widely adopted to interpret the GRB high energy afterglow data (e.g., Kumar & Barniol Duran 2009; Gao et al. 2009; Ghisellini et al. 2010; He et al. 2011; Ackermann et al. 2013; c.f., Tam et al. 2012).

To produce the  $\geq 0.1$  GeV afterglow emission, the synchrotron-radiating electrons should have a random Lorentz factor larger than

$$\begin{aligned}\bar{\gamma}_e &\sim 10^7 \Gamma_2^{-1/2} B^{-1/2} (1+z)^{1/2} \\ &\sim 5.6 \times 10^6 \epsilon_{B,-2}^{-1/4} E_{k,54}^{-1/8} n_0^{-1/8} t_2^{3/8} [(1+z)/1.34]^{1/8} (1)\end{aligned}$$

where  $\Gamma \sim 150 E_{k,54}^{1/8} n_0^{-1/8} t_2^{-3/8} [(1+z)/1.34]^{3/8}$  is the bulk Lorentz factor of the forward shock and  $B \sim 2.8 \text{ Gauss } \epsilon_{B,-2}^{1/2} E_{k,54}^{1/8} n_0^{3/8} t_2^{-3/8} [(1+z)/1.34]^{3/8}$  is the strength of shock-generated magnetic field (Piran 1999), and  $\epsilon_B$  ( $\epsilon_e$ ) is the fraction of the shock energy given to the magnetic field (electrons).

The inverse Compton cooling is in the Klein-Nishina regime and thus get suppressed if the seed photons are more energetic than

$$\begin{aligned}\bar{\epsilon}_s &\sim m_e c^2 \Gamma / \bar{\gamma}_e \\ &\sim 7 \text{ eV } E_{k,54}^{1/4} \epsilon_{B,-2}^{1/4} t_2^{-3/4} [(1+z)/1.34]^{1/4}.\end{aligned}\quad (2)$$

In most cases except in the presence of a giant optical flare, the power released in the energy range  $\leq \bar{\epsilon}_s$  of afterglow emission or late prompt emission powered by the extended activity of the central engine is expected to be (well) below that of magnetic field in the forward shock region  $\sim 10^{50} \text{ erg s}^{-1} \epsilon_{B,-2} E_{k,54} (1+z)/t_2$ . We hence conclude that *usually the electrons generating GeV synchrotron emission do not suffer from sizable inverse Compton cooling.*

The electrons producing GeV synchrotron radiation are in fast cooling. The fraction ( $f$ ) of the total electron energy given to such extremely energetic electrons can be estimated as  $f \approx (\bar{\gamma}_e^{2-p} - \gamma_M^{2-p})/(\gamma_m^{2-p} - \gamma_M^{2-p})$ , where the shock-accelerated electrons are assumed to have an initial distribution  $dn/d\gamma_e \propto \gamma_e^{-p}$  for  $\gamma_m < \gamma_e < \gamma_M$ , the maximal random Lorentz factor of the shock-accelerated electrons is limited by their energy loss via synchrotron radiation and is estimated by  $\gamma_M \sim 10^8 B^{-1/2}$  (Cheng & Wei 1996), and

$$\gamma_m \sim 4500 E_{k,54}^{1/8} n_0^{-1/8} t_2^{-3/8} \left[ \frac{6(p-2)}{(p-1)} \right] \epsilon_{e,-1} \left[ \frac{(1+z)}{1.34} \right]^{3/8}.$$

The luminosity of GeV synchrotron emission can be estimated by

$$\begin{aligned}L_{\text{GeV,syn}} &\sim f \epsilon_e E_k (1+z)/t \\ &\sim 1.3 \times 10^{50} \text{ erg s}^{-1} f_{-1} \epsilon_{e,-1} E_{k,54} t_2^{-1} \left[ \frac{(1+z)}{1.34} \right] (3)\end{aligned}$$

Let's estimate the count rate. The averaged energy of the synchrotron photons above 100 MeV is

$$\langle E \rangle \sim 100 \text{ MeV } (\beta-1)/(\beta-2) [1 - (\epsilon_{\text{syn,M}}/0.1 \text{ GeV})^{2-\beta}],$$

where  $\epsilon_{\text{syn,M}}$  is given by eq.(5) and  $\beta = (p+2)/2$  is the photon spectral index.

For GRB 130427A, the X-ray and optical afterglow emission suggest that  $p \sim 2.2$  and  $\beta \sim 2.1$ . We then

have  $\langle E \rangle \sim 0.2 - 0.4 \text{ GeV}$  for  $\epsilon_{\text{syn,M}} \sim 1 - 10 \text{ GeV}$ . Hence the count rate of the GeV synchrotron radiation is expected to be

$$\begin{aligned}\dot{N} &\sim L_{\text{GeV,syn}}/4\pi D_L^2 \langle E \rangle \\ &\sim 5 \times 10^{-4} \text{ photon cm}^{-2} \text{ s}^{-1} f_{-1} \epsilon_{e,-1} E_{k,54} t_2^{-1} \left[ \frac{(1+z)}{1.34} \right] \\ &\quad D_{L,27.7}^{-2} \left( \frac{\langle E \rangle}{0.4 \text{ GeV}} \right)^{-1}.\end{aligned}\quad (4)$$

Such a rate seems to be able to account for a good fraction of the observed photon flux presented in Fig.2.

### 3.2. Evidence for inverse Compton radiation

At  $t \sim (243, 256.3, 610.6) \text{ s}$  after the trigger of Fermi-GBM, the photon with an energy  $\sim (95.3, 47.3, 41.4) \text{ GeV}$  was detected, respectively (see Fig.3). The detection of such energetic  $\gamma$ -rays alone imposes a tight constraint on the radiation mechanism. Due to the energy loss via the synchrotron radiation, in the rest frame of the shocked medium there is an upper limit on the energy of the accelerated electrons, so is their synchrotron radiation frequency. The maximal synchrotron radiation frequency reads (e.g., Cheng & Wei 1996)

$$\begin{aligned}\epsilon_{\text{syn,M}} &\sim 100 \text{ MeV } \Gamma (1+z)^{-1} \\ &\sim 11 \text{ GeV } E_{k,54}^{1/8} n_0^{-1/8} t_2^{-3/8} \left[ \frac{(1+z)}{1.34} \right]^{-5/8},\end{aligned}\quad (5)$$

which is well below the energy of photons people observed at  $t \sim (243, 256.3, 610.6) \text{ s}$ , suggesting that these high energy  $\gamma$ -rays should have an inverse Compton radiation origin. Therefore though in section 3.1 we have shown that the count rate of the  $> 100 \text{ MeV}$  emission may be accounted for by the synchrotron radiation of the forward shock electrons alone, part of the high energy afterglow emission does have an inverse Compton radiation origin (see also Fig.4 for a numerical example).

### 3.3. GeV-TeV emission powered by the forward shock electrons inverse-Compton-scattering off prompt emission

For GRB 130427A the prompt X-ray emission was very strong and lasted a few hundred seconds (see Fig.1). Simultaneously, the ultra-relativistic GRB outflow drives energetic blast wave and accelerates a large amount of electrons. Some prompt photons will be up-scattered by the shock-accelerated electrons and get boosted to GeV-TeV energies when cross the forward (possibly also reverse) shock region(s). The resulting high energy  $\gamma$ -rays account for part of the observed GeV emission.

For illustration here we only calculate the high energy emission resulting in the external-inverse-Compton (EIC) scattering process in the second episode of the prompt emission ranging from  $\sim 120 \text{ s}$  to  $\sim 250 \text{ s}$  (Golenetskii et al. 2013). This is because at such a relatively late time the deceleration of the GRB outflow is most likely in the Blandford-McKee self-similar regime (Blandford & McKee 1976) and the forward shock cooling/emission can be calculated in the standard way (Piran 1999). We'd like to also point out that the very different temporal behaviors of the GeV and X-ray/soft

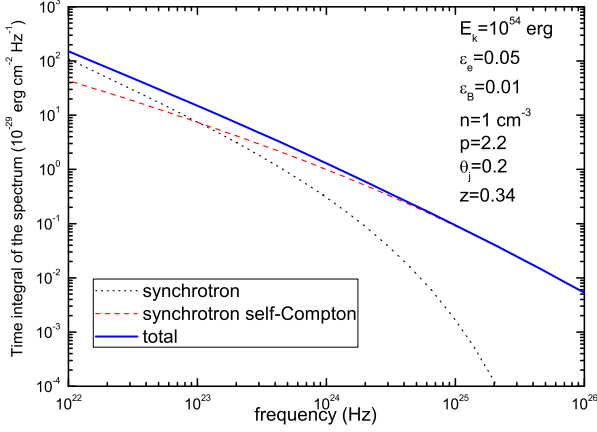


FIG. 4.— The time integral of high energy synchrotron radiation spectrum (the dotted line) and the synchrotron self-Compton radiation spectrum (the dashed line) of a *GRB 130427A*-like burst in the time interval 100 – 400000 s. The initial bulk Lorentz factor of the outflow is taken to be 300. Evidently the sub-GeV emission is sizeably contributed by the forward shock synchrotron radiation while the inverse Compton radiation contributes at higher energies. The total spectrum (the solid line) can be reasonably fitted by  $F_\nu \propto \nu^{-1}$ , which is very similar to the simply-assumed synchrotron radiation spectrum  $F_\nu \propto \nu^{-p/2}$  for  $p \sim 2.2$ , indicating that sometimes the inverse Compton component in the real data may have been improperly interpreted as the high energy part of the synchrotron radiation. The plot is generated from the code developed by Fan et al. (2008).

$\gamma$ -ray emission in such a time interval suggest that these emission are not from the same region.

The inverse Compton scattering is efficient if it is in the Thompson regime, requiring that in the rest frame of the electron the seed photon has an energy smaller than  $m_e c^2$ , i.e., the random Lorentz factor of the electrons should not be higher than

$$\gamma_s \sim \Gamma m_e c^2 / \epsilon_s \sim 1500 \left( \frac{\epsilon_s}{50 \text{ keV}} \right)^{-1} E_{k,54}^{1/8} n_0^{-1/8} t_2^{-3/8} \left[ \frac{(1+z)}{1.34} \right]^{3/8}, \quad (6)$$

where  $\epsilon_s$  is the energy of the seed photon (prompt photon). Therefore, most electrons with a random Lorentz factor  $\sim \gamma_m$  are cooled by the prompt photons at energies

$$\epsilon_s \leq 17 \text{ keV} \left[ \frac{6(p-2)}{(p-1)} \right]^{-1} \epsilon_{e,-1}^{-1}.$$

Such a  $\epsilon_s$  seems to be well below the peak energy  $\sim 240$  keV of the prompt emission in the second episode (Golenetskii et al. 2013). However the total energy released in the energy  $< \epsilon_s \sim 17$  keV is not ignorable since the spectrum is much softer than the typical ones  $F_\nu \propto \nu^0$ . With the observed spectrum  $F_\nu \propto \nu^{-0.6}$  (Golenetskii et al. 2013), we find out that  $\sim 1/3$  of the total energy was released below  $\epsilon_s$ , i.e.,  $\mathcal{F}_{<\epsilon_s} \sim \mathcal{F}/2 \sim 4.5 \times 10^{-5} \text{ erg cm}^{-2} \text{ s}^{-1}$ , where  $\mathcal{F} \sim 9 \times 10^{-5} \text{ erg cm}^{-2}$  is the 20 – 1200 keV energy fluence. The corresponding time-averaged luminosity is  $L_{<\epsilon_s} \sim 10^{50} \text{ erg/s}$ , consistent with the *Swift* data (see Fig.1). Below we estimate the importance of the cooling of forward shock electrons by prompt emission.

In the rest frame of the shocked interstellar medium, the energy density of the seed photons can be estimated as  $U_\gamma \sim L_{<\epsilon_s}/4\pi R^2 \Gamma^2 c \sim 0.3 \text{ erg cm}^{-3} L_{<\epsilon_s,50} E_{k,54}^{-3/4} n_0^{3/4} t_2^{1/4} \left[ \frac{(1+z)}{1.34} \right]^{-1/4}$ , where  $R$  is the radius of the forward shock

$$R \sim 2 \times 10^{17} \text{ cm} E_{k,54}^{1/4} n_0^{-1/4} t_2^{1/4} \left[ \frac{(1+z)}{1.34} \right]^{-1/4}.$$

The comoving energy density of the shock-generated magnetic field is  $U_B \sim 1.35 \text{ erg cm}^{-3} \epsilon_{B,-2} E_{k,54}^{1/4} n_0^{3/4} t_2^{-3/4} \left[ \frac{(1+z)}{1.34} \right]^{3/4}$ . The importance of the inverse Compton cooling caused by the prompt emission is given by the dimensionless parameter  $\mathcal{Y} = U_\gamma/U_B = 0.22 L_{<\epsilon_s,50} E_{k,54}^{-1} \epsilon_{B,-2}^{-1} t_2 \left[ \frac{(1+z)}{1.34} \right]^{-1}$ . Such a small  $\mathcal{Y}$  seems to suggest an unimportant inverse Compton cooling effect. However, as demonstrated below, intriguing radiation is expected.

The number of high energy  $\gamma$ -rays generated by the forward shock electrons inverse-Compton-scattering off prompt emission can be straightforwardly estimated (e.g., Fan et al. 2005b, Gao et al. 2009). The possibility of one seed photon being up-scattered (i.e., the optical depth) in the forward shock region can be estimated as

$$\tau \sim \sigma_T R/3 \sim 4.4 \times 10^{-8} E_{k,54}^{1/4} n_0^{3/4} t_2^{1/4} \left[ \frac{(1+z)}{1.34} \right]^{-1/4}, \quad (7)$$

where  $\sigma_T$  is the Thompson's cross section. The total number of seed photons is

$$N_{\text{seed}} \sim \mathcal{F}_{<\epsilon_s} / <\epsilon_s> \sim 1.5 \times 10^4, \quad (8)$$

where  $<\epsilon_s> \sim 2 \text{ keV}$  is the averaged energy of the seed photons within the energy range of  $\sim 0.3 \text{ keV} - 17 \text{ keV}$  for a spectrum  $F_\nu \propto \nu^{-0.6}$ . The total number of high energy photons detectable for Fermi with an effective area  $S \sim 10^4 \text{ cm}^2$  is

$$N_{\gamma,\text{EIC}} \sim \tau N_{\text{seed}} S \sim 6. \quad (9)$$

The receiving number of scattered photons will be reduced by a factor of  $\sim 0.5$  due to the anisotropic radiation of EIC (Fan & Piran 2008). Hence about  $\sim 3$  high energy  $\gamma$ -rays are expected. The typical energy of the generated high energy  $\gamma$ -rays is expected to be

$$\epsilon_{\text{EIC}} \sim \min\{\gamma_m^2, \gamma_c^2\} <\epsilon_s> \sim 10 \text{ GeV}, \quad (10)$$

where the cooling Lorentz factor of the forward shock electrons reads

$$\gamma_c \sim 2.3 \times 10^3 E_{k,54}^{-3/8} \epsilon_{B,-2}^{-1} n_0^{-5/8} t_2^{1/8} \left( \frac{1+z}{1.34} \right)^{-1/8} \left( \frac{1+Y}{2} \right)^{-1},$$

and  $Y$  is the inverse Compton parameter (including both the synchrotron-self Compton and the EIC radiation).

For GRB 130427A at a redshift  $z = 0.34$ , the optical depth of the universe for 300 GeV-like  $\gamma$ -rays from interactions with photons of the intergalactic background light is expected to be  $\sim 1$  (Gilmore et al. 2012). Therefore whether the tens-GeV photons can be detected or not mainly depends upon their chance of escaping the emitting region. With eq.(13) of Zou et al. (2011) it is straightforward to show that even for 300 GeV photons the optical depth caused by the overlapping of the prompt photons with the forward shock region is  $\sim 2.5 \times 10^{-3}$ , which is so small that can be ignored.

Hence we conclude that the resulting tens-GeV photons can reach us.

*Interestingly, in the time interval  $140 \text{ s} < t < 260 \text{ s}$  in coincidence with the second episode of the prompt emission, five afterglow photons  $> 10 \text{ GeV}$  have been recorded.* Though the synchrotron-self-Compton origin of such photons can not be ruled out considering the somewhat small  $\mathcal{V}$ , the EIC scattering origin due to the overlapping of prompt emission with the forward shock for such a tens-GeV-afterglow-emission enhancement is possible.

#### 4. A POSSIBLE UNIFIED MODEL FOR THE PROMPT SOFT GAMMA-RAY, OPTICAL AND GEV EMISSION OF GRB 130427A, GRB 080319B AND GRB 090902B

Instead of proposing a model dedicated to fit the data of prompt emission of GRB 130427A, we try to outline a unified scenario to understand GRB 130427A, GRB 080319B and GRB 090902B together, motivated by the similarities displayed in the observational features summarized in Tab.2. Please note that  $\alpha_{\text{Band}}$  and  $\beta_{\text{Band}}$  are the low and high energy spectral indexes of the GRBs fitted by the Band function (Band et al. 1992) and  $E_p$  is the observed peak energy of the spectrum.

*Prompt emission from the photosphere.* Prominent thermal radiation components have been identified in the prompt soft- $\gamma$  ray emission of GRB 090902B (e.g., Ryde et al. 2010; Zhang et al. 2011), which is the smoking-gun signature of the photospheric radiation. For GRB 080319B, some people tried to interpret both the ultra-strong soft  $\gamma$ -ray emission and the naked-eye optical flash within the internal shock scenarios (e.g., Kumar & Panaitescu 2008; Li & Waxman 2008; Yu et al. 2009). However, the model of that the prompt optical and soft  $\gamma$ -ray emission are, respectively, the synchrotron and the first-order inverse Compton radiation components of the internal shocks is found to be disfavored (Piran et al. 2009). Moreover, the tight correlation  $\Gamma \propto L^{0.3}$  found in the data analysis of GRBs (Lü et al. 2012; Fan et al. 2012) predicts an extremely low internal shock efficiency unless the slow material shell has a width much wider than that of the fast shell, at odds with the data, where  $L$  is the total luminosity of the outflow. Therefore we suggest that the internal shock origin of the prompt soft  $\gamma$ -ray emission is less likely. One attractive alternative is the so-called photospheric radiation model, in which the GRB prompt emission is mainly from the photosphere but suffers significant modification and its spectrum is normally no longer thermal-like (e.g., Rees & Mészáros 2005; Beloborodov 2010; Lazzati et al. 2011). We adopt such a kind of model for the prompt emission of GRB 080319B and GRB 130427A, and investigate below whether strong prompt optical and GeV emission can be generated.

*Bright optical flash from the synchrotron radiation of internal shocks.* If the prompt emission has a photospheric origin, the internal shocks are likely sub-relativistic since the contrast between the Lorentz factor of the shells is just by a factor of  $\sim 2$ . We denote the bulk Lorentz factor of the fast and slow shells as  $\Gamma_f$  and  $\Gamma_s$ , respectively. The merged shell has a bulk Lorentz factor  $\Gamma_i$ , which is between  $\Gamma_s$  and  $\Gamma_f$ . Therefore the strength of the internal shock satisfies  $\gamma_{\text{in}} < (\Gamma_f/\Gamma_s + \Gamma_s/\Gamma_f) < 1.25$  for  $\Gamma_f \approx 2\Gamma_s$ . The comoving strength of the mag-

netic field in the emitting region can be estimated as  $B_i \sim 100 \text{ Gauss} (\frac{3\epsilon_{\text{B,in}}}{\epsilon_{\text{e,in}}})^{1/2} L_{\text{in},52}^{1/2} R_{i,16}^{-1} \Gamma_{i,2.7}^{-1}$  (Fan & Piran 2008), where  $L_{\text{in}}$  is the luminosity of the internal shock radiation, and  $\epsilon_{\text{e,in}}$  and  $\epsilon_{\text{B,in}}$  are the fractions of the internal shock energy given to the electrons and magnetic field, respectively. The typical synchrotron radiation frequency of the internal shock electrons is  $\nu_m \sim 2.8 \times 10^6 \text{ Hz } \gamma_{\text{m,in}}^2 \Gamma_i B_i / (1+z) \sim 2.2 \times 10^{14} (\gamma_{\text{m,in}}/40)^2 (3\epsilon_{\text{B}}/\epsilon_{\text{e}})^{1/2} L_{\text{in},52}^{1/2} R_{i,16}^{-1} / (1+z) \text{ Hz}$ , where  $\gamma_{\text{m,in}} \sim 40 [6(p-2)/(p-1)](\epsilon_{\text{e}}/0.5)[(\gamma_{\text{in}}-1)/0.2]$ . Following the standard treatment, the synchrotron self-absorption frequency can be estimated as  $\nu_a \sim 1.3 \times 10^{15} \text{ Hz } (\frac{3\epsilon_{\text{B,in}}}{\epsilon_{\text{e,in}}})^{1/2} L_{53}^{2/(p+4)} L_{\text{in},52}^{\frac{p+2}{2(p+4)}} (\frac{\gamma_{\text{m,in}}}{40})^{\frac{2(p-1)}{p+4}} \Gamma_{i,2.7}^{-\frac{2(p+6)}{p+4}} (\frac{\delta t}{0.5 \text{ s}})$ , i.e., above the optical band and then the optical emission is somewhat suppressed. The internal-shock-electrons with random Lorentz factor  $\gamma_e \leq \gamma_{\text{e,kn}} \equiv \Gamma_i m_e c^2 / [(1+z)E_p] \sim 250 \Gamma_{i,2.7} [(1+z)E_p/1 \text{ MeV}]^{-1}$  are mainly cooled by the prompt soft  $\gamma$ -rays (i.e., the EIC process) and the cooling Lorentz factor can be estimated as  $\gamma_{\text{c,in}} \sim 6 R_{i,16} \Gamma_{i,2.7}^3 L_{\gamma,53}^{-1}$  (Fan & Piran 2008), where  $L_{\gamma}$  is the luminosity of the prompt soft  $\gamma$ -ray emission. So the comoving temperature of the emitting region is  $kT_i \sim \min\{\gamma_{\text{m,in}}, \gamma_{\text{c,in}}\} m_e c^2$  and the prompt optical flux density can be estimated as (Zou et al. 2009)

$$f_{\nu_{\text{opt}}} \sim \frac{2\pi\nu_{\text{opt}}^2 (1+z)^3 \Gamma_i kT_i}{c^2} \left(\frac{R_i}{\Gamma_i D_L}\right)^2 \\ \sim 3.4 \text{ Jy } \nu_{\text{opt},14.7}^2 \Gamma_{i,2.7}^{-1} R_{i,16}^2 \\ \left(\frac{\min\{\gamma_{\text{m,in}}, \gamma_{\text{c,in}}\}}{6}\right) \left(\frac{1+z}{2}\right)^3 D_{L,28.3}^{-2} \quad (11)$$

For reasonable parameters of GRB 080319B and GRB 130427A (i.e.,  $\Gamma_i \sim 500 - 1000$  and  $R_i \sim 10^{16} \text{ cm}$ ), very bright optical flashes are expected, consistent with the data.

*Energetic GeV emission from the EIC radiation of internal shocks.* As a result of the overlapping of the prompt emission and the optical radiation region, the electrons will scatter off the prompt emission and then produce high energy emission with a luminosity  $\sim L_{\text{in}}$  (Beloborodov 2005; Zou et al. 2009). The EIC radiation flux peaks at  $\sim \min\{\gamma_{\text{m}}^2, \gamma_{\text{c}}^2\} E_p \sim 100 \text{ MeV}$  and the spectrum  $F_{\nu} \propto \nu^{-p/2}$  can extend up to the energy  $\sim (\Gamma_i m_e c^2)^2 / [(1+z)^2 E_p] \sim 0.25 \text{ TeV } \Gamma_{i,3}^2 (E_p/1 \text{ MeV})^{-1} (1+z)^{-2}$ , as observed in GRB 090902B and GRB 130427A. Adopting eq.(13) of Zou et al. (2011), it is straightforward to show that the tens-GeV photons can escape without being significantly absorbed by the prompt  $\gamma$ -rays.

#### 5. SUMMARY

GRB 130427A was simultaneously detected by five  $\gamma$ -ray space telescopes and by three RAPTOR full-sky persistent monitors. The isotropic-equivalent energy of the prompt emission is  $\sim 10^{54} \text{ erg}$  and the absence of a jet break in the X-ray lightcurve up to  $t > 7 \text{ days}$  suggests a geometry-corrected  $\gamma$ -ray energy release of  $> 10^{52} \text{ erg}$ , rendering it one of the most powerful GRBs detected so far. At a redshift of 0.3399, the very high energy emission ( $\leq 300 \text{ GeV}$ ) from GRB 130427A will not be



TABLE 2  
GENERAL FEATURES OF GRB 080319B, GRB 090902B AND GRB 130427A.

| Quantity                    | GRB 080319B              | GRB 090902B                   | GRB 130427A                   |
|-----------------------------|--------------------------|-------------------------------|-------------------------------|
| $\alpha_{\text{Band}}$      | $0.833 \pm 0.014$        | $0.61 \pm 0.01$               | $0.789 \pm 0.003^a$           |
| $\beta_{\text{Band}}$       | $3.499 \pm 0.364$        | $3.8 \pm 0.25$                | $3.06 \pm 0.06^a$             |
| $E_p$                       | $651 \pm 15$ keV         | $726 \pm 8$ keV               | $830 \pm 5$ keV $^a$          |
| $z$                         | 0.937                    | 1.822                         | 0.3399                        |
| $E_{\gamma, \text{iso}}$    | $1.3 \times 10^{54}$ erg | $4 \times 10^{54}$ erg        | $1.05 \times 10^{54}$ erg     |
| Duration of prompt emission | 57 s                     | 26 s                          | $\sim 138$ s $^b$             |
| prompt optical emission     | $\sim 20$ Jy             | no observation                | $\sim 4$ Jy                   |
| prompt GeV emission         | no observation           | $\sim 10^{-4}$ erg cm $^{-2}$ | $\sim 10^{-4}$ erg cm $^{-2}$ |
| main references             | 1                        | 2,3                           | 4,5,6,7                       |

$^a$  The time-averaged spectrum of the main phase of the burst (from  $T_0 + 0.002$  s to  $T_0 + 18.432$  s) measured by Fermi-GBM (Kienlin et al. 2013).

$^b$  Most of the energy was released in the first  $\sim 18$  s.

—References: (1) Racusin et al. 2008; (2) Abdo et al. 2009b; (3) Cucchiara et al. 2009; (4) Kienlin et al. 2013; (5) Zhu et al. 2013b; (6) Amati et al. 2013; (7) Wren et al. 2013.

considerably attenuated by the cosmic infrared/optical background. Together with the fact this nearby GRB is super-luminous, it is very favorable to detect the very high energy emission (Xue et al. 2009). The detection of four photons above 40 GeV (two above 70 GeV) by Fermi-LAT is in agreement with such a speculation.

The emission above 100 MeV lasted about one day (see Fig.2). As firstly demonstrated by Zou et al. (2009), for bursts as energetic as GRB 080319B, the forward shock synchrotron radiation may be the dominant component of the afterglow emission below  $\sim$  a few GeV while the inverse Compton radiation mainly contributes at higher energies. For GRB 130427A, the sub-GeV emission may be dominated by the forward shock synchrotron radiation while the inverse Compton radiation mainly produce GeV-TeV emission (see Fig.4 for a numerical example). In particular, for the photons with energies  $\sim$  (95.3, 47.3, 41.4) GeV detected at  $t \sim$  (243, 256.3, 610.6) s (see Fig.3), the forward shock synchrotron radiation model has been convincingly ruled out and an inverse Compton radiation origin is needed. We also find out that the external-inverse-Compton-scattering of the prompt emission (the second episode, i.e.,  $t \sim 120 - 260$  s) by the forward-shock-accelerated electrons is expected to produce a few  $\gamma$ -rays with a typical energy  $\sim 10$  GeV, which may account for some  $\gamma$ -rays at energies  $> 10$  GeV detected in the same time interval.

We have also outlined a possible unified model for the prompt soft  $\gamma$ -ray, optical and GeV emission of GRB 130427A, GRB 080319B and GRB 090902B. In such a model the prompt soft  $\gamma$ -rays are mainly the photospheric radiation, while the subsequent internal shocks produce bright optical flash via synchrotron radiation and energetic GeV flash via the EIC scattering (see Section 4).

The IceCube collaboration reported their null detec-

tion of  $> 1$  TeV neutrinos in spatial and temporal coincidence with GRB 130427A (Blaufuss 2013). Such a result is a bit disappointed but not unexpected. For example, in the internal shock model, no detectable neutrino is expected if the proton spectrum is as soft as the electron spectrum (i.e.,  $dn/d\epsilon \propto \epsilon^{-4}$ , as inferred from the prompt MeV emission). Only for the proton spectrum as hard as  $dn/d\epsilon \propto \epsilon^{-2}$ , significant detection (i.e., about one event at PeV energies) by IceCube is possible. The high energy prompt emission does suggest such a hard spectrum. However it is likely powered at a radius  $R_i \sim 10^{16}$  cm (see Section 4), which is too large for efficient pion production.

Finally we'd like to mention that the detection of one LAT photon of energy  $\sim 72$  GeV at  $t \sim 18.6$  s after the Fermi-GBM trigger of GRB 130427A can also be used to constrain the possible variation of the speed of light arising from quantum gravity effects. However, the limit is weaker than that set by the detection of one 31 GeV photon at  $t \sim 0.73$  s after the trigger of GRB 090510 (Abdo et al. 2009a).

#### ACKNOWLEDGMENTS

We are grateful to Dr. Y. C. Zou, L. Shao and D. Xu for helpful discussion. This work was supported in part by 973 Program of China under grants 2009CB824800 and 2013CB837000, National Natural Science of China under grants 11173064 and 11273063, and by China Postdoctoral science foundation under grant 2012M521137. YZF is also supported by the 100 Talents program of Chinese Academy of Sciences and the Foundation for Distinguished Young Scholars of Jiangsu Province, China (No. BK2012047). PHT is supported by the National Science Council of the Republic of China (Taiwan) through grant NSC101-2112-M-007-022-MY3.

#### REFERENCES

- Abdo, A. et al. 2009a, *Nature*, 462, 331  
 Abdo A. et al. 2009b, *ApJ*, 706, L138  
 Abdo A. et al. (Fermi collaboration) 2013, arXiv:1303.2908  
 Ackermann, M. et al. 2013, *ApJ*, 763, 71  
 Acciari, V. A. et al. (VERITAS collaboration) 2011, *ApJ*, 732, 62  
 Aharonian, F., et al. (H.E.S.S. collaboration) 2009, *A&A*, 495, 505  
 Albert, J., et al. (MAGIC collaboration) 2007, *ApJ*, 667, 358  
 Amati, L., Della Valle, M., Frontera, F., Malesani, D., Guidorzi, C., Montanari, E., & Pian, E. 2007, *A&A*, 463, 913  
 Amati, L., Dichiara, S., Frontera, F., & Guidorzi, C. 2013, *GCN Circ.* 14503 (<http://gcn.gsfc.nasa.gov/gcn3/14503.gcn3>)  
 Band D. et al., 1993, *ApJ*, 413, 281  
 Barthelmy, S. D. et al. 2013 *GCN Circ.* 14470 (<http://gcn.gsfc.nasa.gov/gcn3/14470.gcn3>)  
 Beloborodov, A. M. 2005, *ApJ*, 618, L13  
 Beloborodov, A. M. 2010, *MNRAS*, 407, 1033  
 Blandford, R. D., & McKee, C. F., 1976, *Phys. Fluids*, 19, 1130

- Blaufuss, E. (IceCube collaboration) 2013, GCN Circ. 14520 (<http://gcn.gsfc.nasa.gov/gcn3/14520.gcn3>)
- Cheng, K.S., & Wei, D.M., 1996, MNRAS, 283, L133
- Cucchiara, A., Fox, D. B., Tanvir, N., & Berger, E., 2009, GCN 9873
- Evans, P. A., et al. 2009, MNRAS, 397, 1177
- Fan, Y. Z. & Piran, T. 2008, Front. Phys. China., 3, 306
- Fan, Y. Z., Piran, T., Narayan, R., & Wei, D. M. 2008, MNRAS, 384, 1483
- Fan, Y. Z., Wei, D. M., Zhang, F. W., & Zhang, B. B. 2012, ApJL, 755, L6
- Fan, Y. Z., Zhang, B., & Wei, D. M. 2005a, ApJ, 629, 334
- Fan, Y. Z., Zhang, B., & Wei, D. M. 2005b, MNRAS, 361, 965
- Flores, H. et al., 2013, GCN Circ. 14491 (<http://gcn.gsfc.nasa.gov/gcn3/14491.gcn3>)
- Gao, W. H., Mao, J. R., Xu, D., & Fan, Y. Z., 2009, ApJ, 706, L33
- Ghisellini, G., Ghirlanda, G., Nava, L., & Celotti, A. 2010, MNRAS, 403, 926
- Gilmore, R., Somerville, R., Primack, J., & Domínguez, A. 2012, MNRAS, 422, 3189
- Golenetskii, S., et al. 2013, GCN Circ. 14487 (<http://gcn.gsfc.nasa.gov/gcn3/14487.gcn3>)
- Goodman J., 1998, ApJ, 308, L47
- He, H. N., Wu, X. F., Toma, K., Wang, X. Y., & Mészáros, P. 2011, ApJ, 733, 22
- Holland, S. T., et al. 2010, ApJ, 717, 223
- Horan, D., et al. 2007, ApJ, 655, 396
- Hurley, K. et al. 1994, Nature, 372, 652
- Jarvis, A. et al. 2010, ApJ, 722, 862
- Kumar, P., & Panaitescu, A. 2008, MNRAS, 391, L19
- Kumar, P., & Barniol Duran, R. 2009, MNRAS, 400, L75
- Lazzati, D., Morsony, B. J., & Begelman, M. C. 2011, ApJ, 732, 34
- Levan, A. J., Cenko, S. B., Perley, D. A., & Tanvir, N. R. 2013, GCN Circ. 14455 (<http://gcn.gsfc.nasa.gov/gcn3/14455.gcn3>)
- Li, Z., & Waxman, E., 2008, ApJ, 674, L65
- Lü, J. et al. 2012, ApJ, 751, 49
- Mészáros, P. 2002, Ann. Rev. Astron. Astrophys., 40, 137
- Maselli, A., Beardmore, A. P., Lien, A. Y., Mangano, V., Mountford, C. J., Page, K. L., Palmer, D. M., & Siegel, M. H. 2013, GCN Circ. 14448 (<http://gcn.gsfc.nasa.gov/gcn3/14448.gcn3>)
- Piran, T. 1999, Phys. Rep., 314, 575
- Piran T., Sari R., Zou Y. C., 2009, MNRAS, 393, 1107
- Pozanenko, A., Minaev, P., & Volnova, A. 2013, GCN Circ. 144484 (<http://gcn.gsfc.nasa.gov/gcn3/14484.gcn3>)
- Racusin, J. L., et al. 2008, Nature, 455, 183
- Rees, M. J. & Mészáros, P. 2005, ApJ, 628, 847
- Ryde, F., et al. 2010, ApJ, 709, L172
- Tam, P. H. T., Kong, A. K. H., & Fan, Y. Z. 2012, ApJ, 754, 117
- von Kienlin, A., 2013, GCN Circ. 14473 (<http://gcn.gsfc.nasa.gov/gcn3/14473.gcn3>)
- Verrecchia, F., et al. 2013, GCN Circ. 14515 (<http://gcn.gsfc.nasa.gov/gcn3/14515.gcn3>)
- Wang, X. Y., Li, Z., & Mészáros, P., 2006, ApJ, 641, L89
- Wren, J., Vestrand, W. T., Wozniak, P., & Davis, H. 2013, GCN Circ. 14476 (<http://gcn.gsfc.nasa.gov/gcn3/14476.gcn3>)
- Xu, D., et al. 2013, GCN Circ. 14478 (<http://gcn.gsfc.nasa.gov/gcn3/14478.gcn3>)
- Xue, R. R., et al. 2009, ApJ, 703, 60
- Yu, Y. W., Wang, X. Y., & Dai, Z. G., 2009, ApJ, 692, 1662
- Zhang, B., & Meszaros, P. 2004, Int. J. Mod. Phys. A, 19, 2385
- Zhang, B. B., et al., 2011, ApJ, 730, 141
- Zhang, B. B., et al., 2012a, ApJ, 756, 190
- Zhang, F. W., Shao, L., Yan, J. Z., & Wei, D. M. 2012b, ApJ, 750, 88
- Zheng, W. K., Cenko, S. B., Filippenko, A. V., & Morgan, A. 2013, GCN Circ. 14525 (<http://gcn.gsfc.nasa.gov/gcn3/14525.gcn3>)
- Zhu, S., Racusin, J., Kocevski, D., McEnery, J., Longo, F., Chiang, J., & Vianello, G. 2013a, GCN Circ. 14471 (<http://gcn.gsfc.nasa.gov/gcn3/14471.gcn3>)
- Zhu, S., Racusin, J., Kocevski, D., McEnery, J., Longo, F., Chiang, J., & Vianello, G. 2013b, GCN Circ. 14508 (<http://gcn.gsfc.nasa.gov/gcn3/14508.gcn3>)
- Zou, Y.C., Fan, Y.Z., & Piran, T., 2009, MNRAS, 396, 1163
- Zou, Y.C., Fan, Y.Z., & Piran, T., 2011, ApJ, 726, L2